Polymer 49 (2008) 5446–5451

Contents lists available at ScienceDirect

Polymer

journal homepage: www.elsevier.com/locate/polymer

Gaseous infiltration method for preparation of three-dimensionally ordered macroporous polyethylene

Xu Zhang, Weidong Yan*, Huifang Yang, Binyuan Liu, Haiqing Li

Institute of Polymer Science and Engineering, Hebei University of Technology, Tianjin 300130, China

ARTICLE INFO

Article history:
Received 27 May 2008
Received in revised form
18 September 2008
Accepted 25 September 2008
Available online 10 October 2008

Keywords:
Ordered macroporous polymer
Polyethylene
Templates supported catalysts

ABSTRACT

Three-dimensionally ordered macroporous polyethylenes (3DOM PE) with pore size ranging from 135 nm to 410 nm were prepared using supported catalysts on the surface of silica microsphere as template, followed infiltration of gaseous ethylene and polymerization. The morphology of 3DOM PE was characterized by SEM and the reflectance spectrum was recorded by UV–vis. It is shown that the pores are uniform, flexible and arranged in a highly ordered fashion. Reflectance spectrum of 3DOM PE also provided verification of the uniform nature of the sample. Moreover, the effect of confined space on polymerization was investigated by GPC and DSC. The results indicate that the porous PE possesses higher M_w compared with bulk PE, and exhibits lower melting temperature and crystallinity than those of bulk PE.

© 2008 Elsevier Ltd. All rights reserved.

1. Introduction

Increasing attention has been placed on the creation of three-dimensionally ordered macroporous (3DOM) materials due to their potential applications in photonic crystals [1–4], sensors [5–8], separation and adsorbent media [9,10], catalytic surfaces and supports [11–14], and chromatographic materials [15–17]. A variety of porous materials such as metals [18,19], inorganic materials [20–22], semiconductors [23,24] and polymers [25–32] have been fabricated by replicating colloidal crystal templates. Fabrication based on this approach is remarkable due to its simplicity, its fidelity in transferring the structure from the template to the replica, and precise control the size of the pores and the periodicity [33]. Comparing metals and inorganic macroporous materials, macroporous polymer materials have attracted more interests, because they are flexible, liable to functional design, and facile to prepare. So far, many 3DOM polymers have been prepared and applied in above-mentioned application fields [25–32,34–36].

Scanning the whole procedure for the preparation of 3DOM polymers using the colloidal template method, the key point lies in the design of the method of the filling precursors into interstices of colloidal crystals, which can have a significant effect on the final structure and performances of resulting materials [33]. As far as the preparation of 3DOM polymer is concerned, most of previous preparation methods attempted to use liquid monomer as precursors *via* radical polymerization or crosslink by thermal treatment or exposure to UV light [37–40], due to the limitation of monomers and polymerization methods. However, it still remains a great challenge in using more available infiltration and polymerization methods to fabricate other polymer materials by template-directed synthesis.

Use of gaseous phase as the precursors have some advantages to use gaseous phase as the precursors, such as filling rapidly, and solvent can be avoidable, which can increase the filling defects when the solvent was removed. Despite these advantages, to the best of our knowledge there is only chemical vapor deposition (CVD) [41–43], using gaseous phase as the precursors. Nevertheless, CVD method is in need of harsh conditions and limited to fabricate inorganic 3DOM materials. For example, Blanco et al. [43] fabricated 3DOM Si by means of CVD using disilane gas as a precursor, whose deposition temperature is varied from 250 °C for low filling fractions to 350 °C for high ones. Thus, a kind of infiltration and polymerization easily available to construct the 3DOM polymer by template-directed method is very expectant.

Ethylene gaseous polymerization is well known in industry catalyzed by catalyst supported on silica, which provide a possibility to fabricate 3DOM PE using gas ethylene as a precursor. The cases encourage us to fabricate 3DOM polyethylene (3DOM PE) *via* gaseous phase infiltration of silica crystal templates. This method to fabricate 3DOM PE gives the following advantages: 1) the organic solvent is ignored in the fabrication process, which is more friendly to environment; 2) the important procedure of peeling off bulk polymer from the surface of composites during the typical preparation of 3DOM polymer is more convenient than that of in solution

---

* Corresponding author. Tel.: +86 022 26564866; fax: +86 022 26582421.
E-mail address: yanwd@hebut.edu.cn (W. Yan).

0032-3861/$ – see front matter © 2008 Elsevier Ltd. All rights reserved.
doi:10.1016/j.polymer.2008.09.064

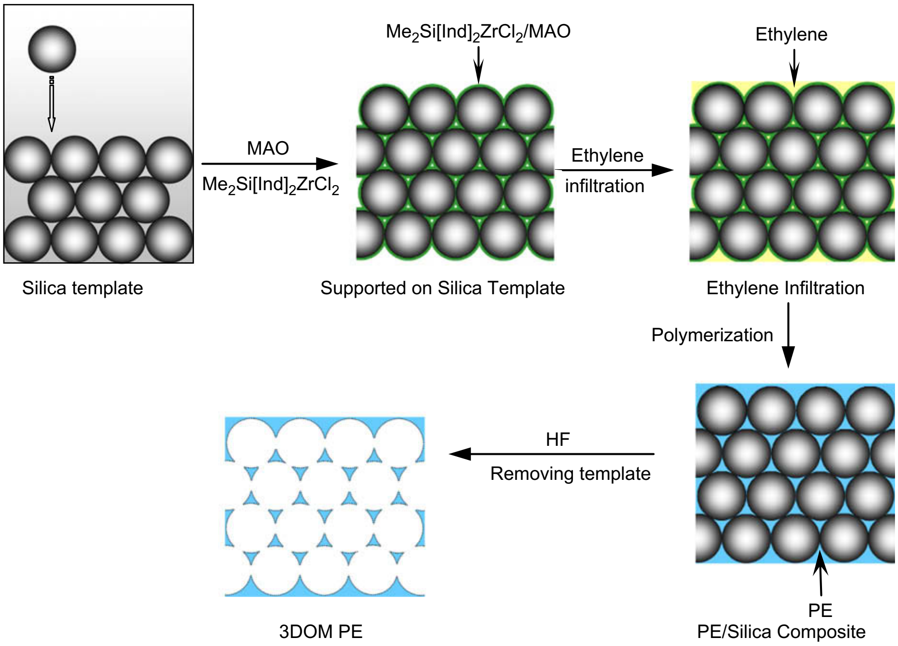

Scheme 1. Schematic diagram for fabricating 3DOM polyethylene by gaseous infiltration method.

polymerization; 3) 3DOM PE with uniform pores and decrease of the filling defects were obtained under efficient filling; 4) also, it can be extended to using other gaseous phase olefins to fabricate 3DOM polyolefin by this method, such as 3DOM polypropylene and 3DOM polyisobutene.

Herein, three-dimensionally ordered macroporous polyethylenes (3DOM PE) with pore size ranging from 135 to 410 nm, arranged in a highly ordered fashion were reported using convenient gaseous phase infiltration of silica crystal template strategy. The process is described in Scheme 1. Resulting PEs obtained from confined three-dimensionally ordered space were measured by GPC and DSC.

2. Experimental

2.1. Materials

Ethanol, 25 wt.-% aqueous ammonia, and 40 wt.-% hydrofluoric acid (HF) purchased from Tianjin Chemical Reagent Factory are reagent quality without further purification. Toluene was refluxed and distilled from Na–benzophenone under dry nitrogen before use. Tetraethoxysilane was commercially obtained from Beijing Chemical Limited Company. Methylaluminoxane (MAO, 10% solution in toluene) was purchased from Arbemarle Company. $Me_2Si[Ind]_2ZrCl_2$ and ethylene were supplied by Yansan Sinopec company and used without further purification. Monodispersed silica templates with average diameter 190 nm, 275 nm and 520 nm were prepared according to Stöber–Fink–Bohn technique [44]. The resulting pellets were sintered at 600 °C for 2 h to enhance the connectivity between the spheres and then cooled down to ambient temperature for further use as templates.

2.2. Supporting procedures

The silica template was treated under vacuum for 2 h at 120 °C, then cooled under argon and placed in the Schlenk flask. MAO solution (5 ml) was injected into the flask under vacuum and kept at 60 °C for 9 h, and then the solution was removed. After washing with purified toluene for five times, the modified silica template was dried under vacuum. $Me_2Si[Ind]_2ZrCl_2$ (15.0 mg) was dissolved in 5.0 ml of purified toluene at 35 °C. Afterwards, the solution was injected into the flask loaded with silica template supported MAO under vacuum and stirred slowly at 60 °C for 9 h. After removing the solution, the resulting solid was washed for three times with 10 ml toluene every time, and dried under vacuum, then saved under argon protection.

2.3. Preparation of 3DOM PE

The Schlenk flask loaded with silica template supported catalyst was heated to the desired temperature (60 °C). Then the flask was degassed, followed by continuous introduction of ethylene gas flow at 0.1 MPa pressure. The polymerization was carried out for 2 h at a constant temperature of 60 °C. The reaction was

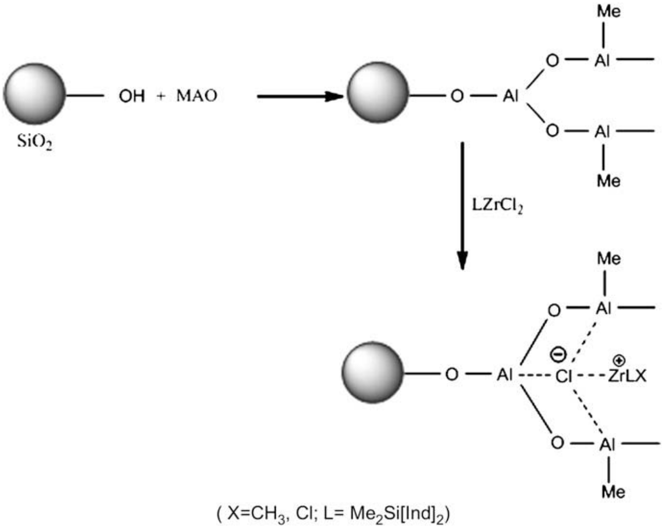

Scheme 2. Supported reaction on the surface of silica microsphere.

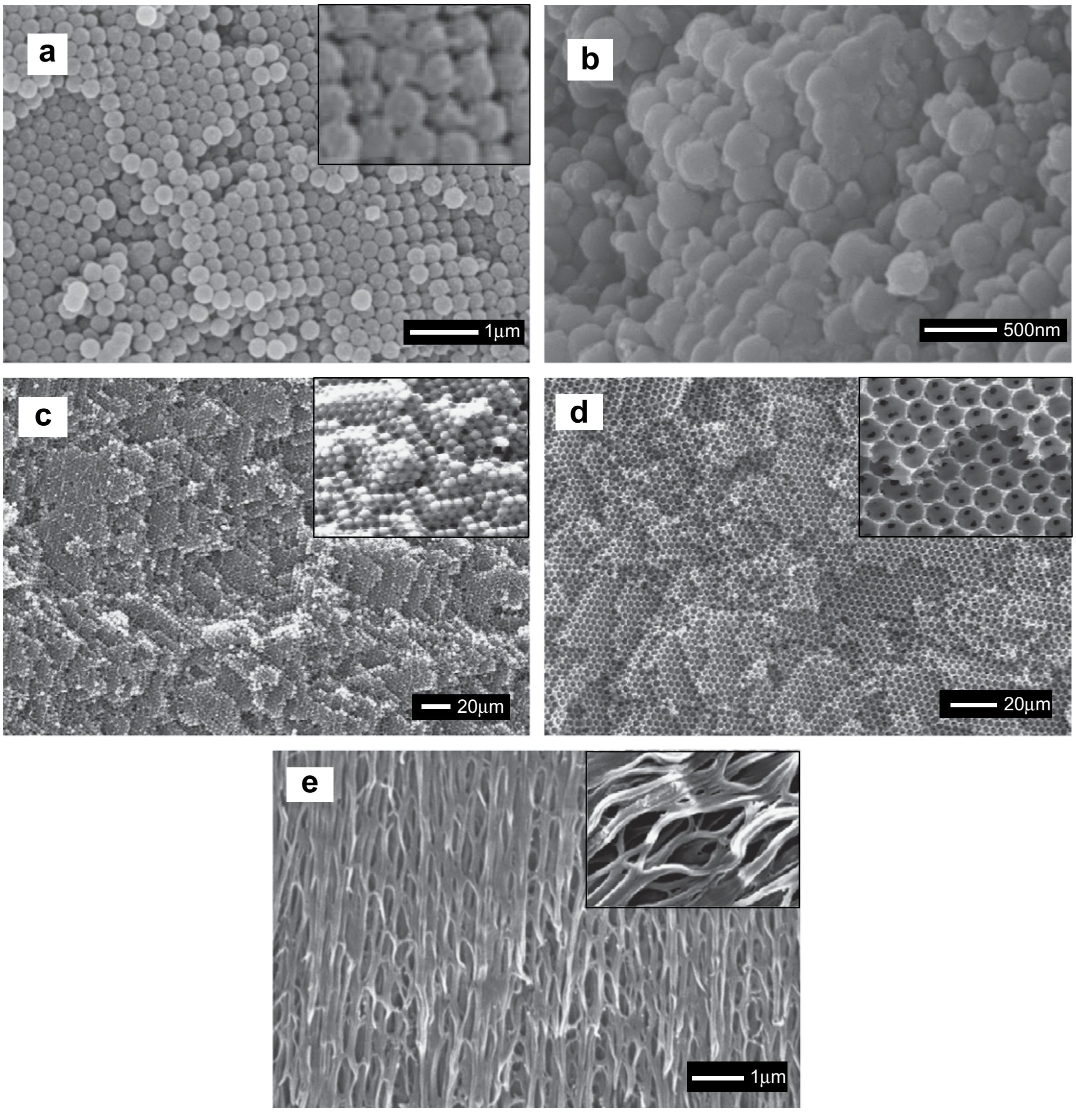

Fig. 1. SEM images of (a) silica template supported with MAO/$Me_2Si[Ind]_2ZrCl_2$ catalytic system (the content of Zr is 0.14 wt.-%; diameter of silica microsphere: 275 nm), (b) silica template supported with MAO/$Me_2Si[Ind]_2ZrCl_2$ catalytic system (the content of Zr is 1.2 wt.-%; the same diameter with (a)), (c) PE/SiO_2 composite, (d) 3DOM PE fractured in liquid nitrogen (diameter: 210 nm), and (e) 3DOM PE incised at ambient temperature.

terminated with acidified ethanol, and the product was the composite of PE/silica. The composite was treated with 10% HF solution for 10 min under ultrosonication and soaked overnight. Thus, 3DOM PE was obtained. The resulting 3DOM PE was washed with distilled water until neutral and dried at 80 °C under vacuum.

2.4. Characterization

The content of Zr supported on silica template was measured by spectrophotometric method (model Cary300 UV–Vis Spectrophotometer). The vacuum-sputtered samples with Au were characterized using scanning electron microscopy (Hitachi S-530 SEM). In the SEM images, over 100 spheres or pores were measured to determine their average diameters. The diffuse reflectance spectrum of 3DOM PE was recorded by Cary300 UV–Vis equipped with diffuse reflectance accessory (DRA-CA-30I), the range of incidence light 350–900 nm was used to measure the reflectance spectrum and the size of 3DOM PE sample is $1 \times 0.5\ cm^2$. GPC measurements were carried out *via* PL-GPC-220 in trichloro-benzene (TCB) at 140 °C. Differential scanning calorimetric (DSC) analysis was performed on a Perkin–Elmer DSC at a heating rate of 10 °C/min under nitrogen from ambient temperature to 150 °C. The level of crystallinity of PE sample was determined by comparing the heat of fusion for a PE sample to the heat of fusion for the completely crystallized PE sample.

3. Results and discussion

Several procedures have been described to support metallocenes on silica [45–52]. According to a report by Chen and coworkers [53], the process used to prepare the Zr/SiO_2 catalyst probably involves the following reactions (Scheme 2): the treatment of SiO_2 with MAO most certainly caused the reaction of surface hydroxyls with AlMe groups in MAO to evolve methane. Those AlMe groups not attached on silica can elicit an anionic ligand from the zirconocene precursor to form the zirconocenium species to initiate PE polymerization. As later demonstrated, the content of Zr had significant influence on the fabrication of 3DOM PE. Proper content of Zr is essential for achieving perfect 3DOM PE. The excess Zr will obstruct the infiltration of gaseous monomers

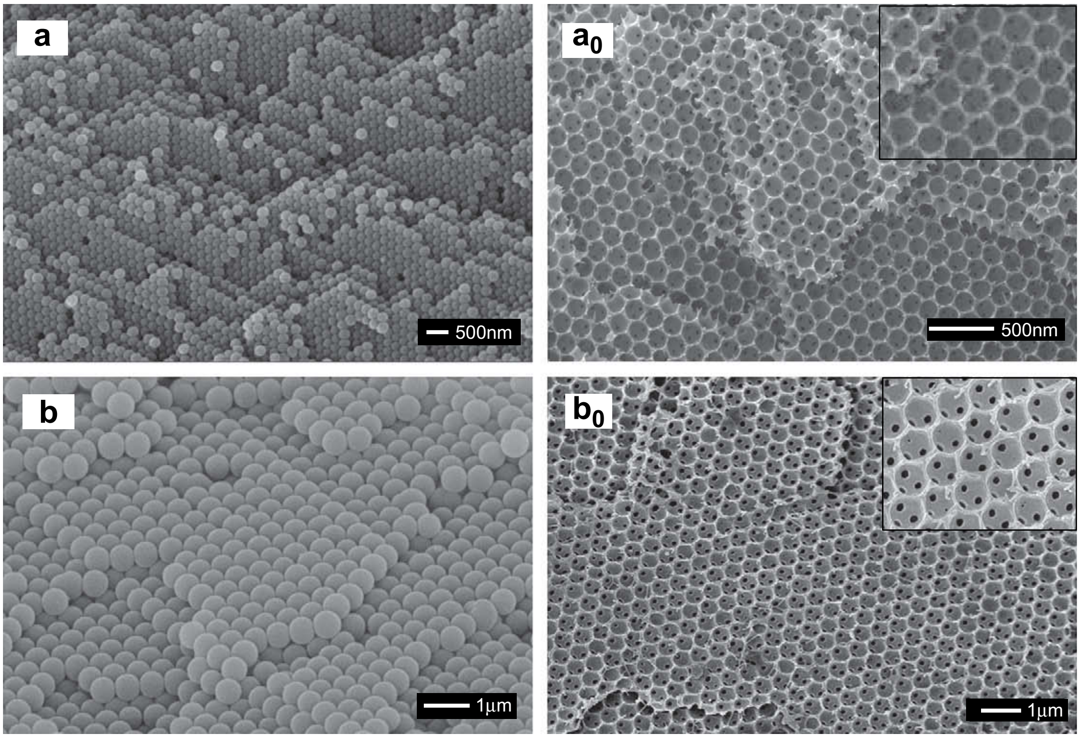

Fig. 2. SEM images of the templates with varied sphere sizes: (a) 190 nm, (b) 520 nm, and the corresponding 3DOM PE: (a_0) 135 nm, (b_0) 410 nm.

into the interstitial voids of silica template and result in defective 3DOM PE.

Fig. 1a and b depicts SEM images of sintered silica templates loaded with different Zr contents. Comparing Fig. 1a (the content of Zr is 0.14 wt.-%) with b (the content of Zr is 1.2 wt.-%), it is obvious that the higher content of Zr blocks the interstitial voids of silica template, which possibly results in the monomer incomplete infiltration into the voids, consequently, the defects would be formed in the 3DOM polymer. Therefore, sintered silica template loaded with proper content of Zr was selected as template to prepare the 3DOM PE. Fig. 1c shows the morphology of the composite of PE/silica, the spherical voids in the sample are all matched with the size of starting silica template and maintained their three-dimensional closed-packed structures, and it is observed that some wire drawing appear on the surface of section, they were generated during the procedure of fracture. As illustrated by Fig. 1d, filling defects are greatly reduced, and the pores have a periodic structure complementary to that of an opal – each of them in a highly ordered fashion. At high magnifications shown in inset of Fig. 1d, it is clearly seen that each pore is connected to its twelve neighbors by a small "window". The center-to-center distances between air microspheres in the resulting 3DOM PE are about 210 nm, which are smaller than that of the pristine silica template. This indicates that the 3DOM PE shrinks approximately 24% after removal of rigid silica template. Fig. 1e shows the fracture section of 3DOM PE (same sample as in Fig. 1c), which was incised at ambient temperature. The ordered pores transformed into "net", indicating that the 3DOM PE inherits the flexible property of polyethylene.

Moreover, 3DOM PEs with different pore sizes were fabricated using the different silica templates by this method, the morphologies of the fractured silica templates with different sizes are shown in Fig. 2a and b, the corresponding 3DOM PE are shown in Fig. 2a_0 and b_0 as well. The pore sizes of corresponding 3DOM PEs shrinked compared with average diameter of the silica templates. The results for preparation of 3DOM PE were summarized in Table 1, revealing that the contraction increased with decreasing average

Table 1
The results for preparation of 3DOM PE.

Sample	Particle diameter of silica template (nm)	Zr loading (wt.-%)	Pore diameter of 3DOM PE (nm)	Shrinkage (%)
3DOM PE-1	190	0.21	135	30
3DOM PE-2	275	0.14	210	24
3DOM PE-3	520	0.12	410	21

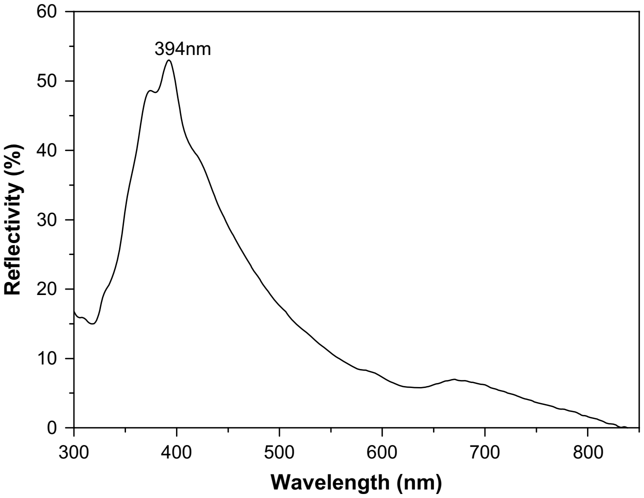

Fig. 3. Typical reflectance spectrum of 3DOM PE sample: PE-2 sample (the pore diameter is 210 nm).

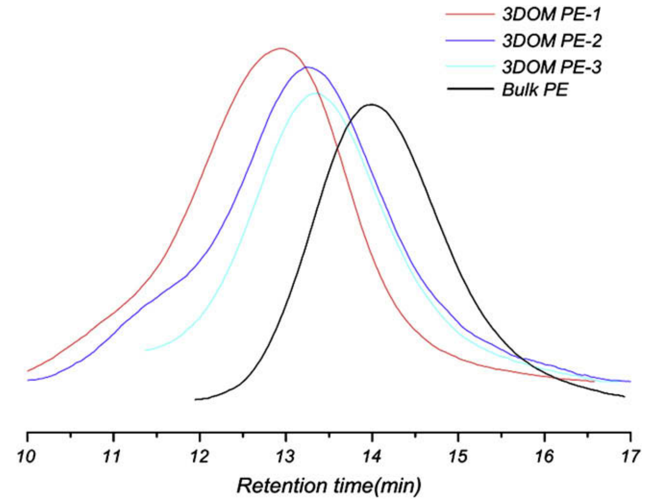

Fig. 4. GPC curves of bulk PE sample and the 3DOM PE samples with different pore sizes.

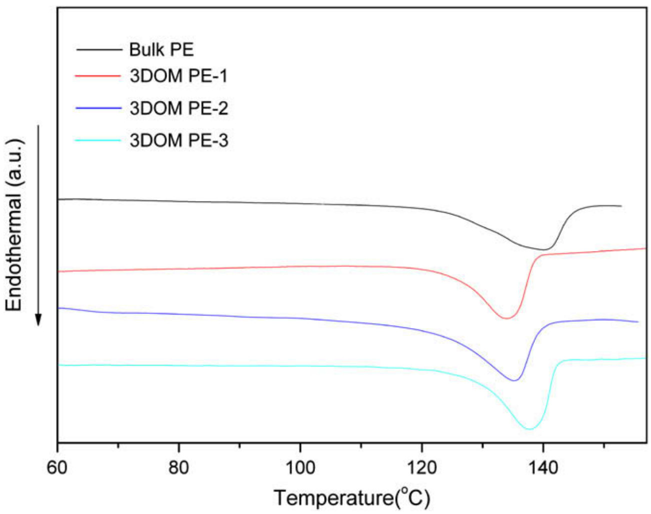

Fig. 5. DSC scans for the bulk PE and the 3DOM PE samples with different pore sizes.

diameter of silica microspheres. The pore diameter contraction after removal of the rigid template is common in the preparation of 3DOM polymers [34–36,54,55], and can be explained in terms of confinement effect of the polymer chains. When the coordination polymerization occurs in the small space between the rigid silica microspheres, the polymer chains are strongly confined, which results in accumulation of internal stress. Once the confinement effect is weakened by removal of template, the internal stress is released accompanied by the elastic recovery of the polymer chains. This leads to decrease of the pore size. From Table 1, it can be found that with the decrease of the diameter of the silica microsphere, the confinement effect on the polymer chains gets more drastic, which results in the shrinkage of 3DOM PE increasing.

As analogous to some reported 3DOM polymers [2,26–29,39], the 3DOM PE also exhibits optical characterization. The typical reflectance spectrum of 3DOM PE-2 is shown in Fig. 3. The reflectance spectrum exhibits a broad peak with a center wavelength of 394 nm, which indicates the diffractive properties of the matrix and the high crystalline quality of this sample [2].

The effects of confined space on the chain sizes and thermal properties of 3DOM PE were also investigated by GPC and DSC. Fig. 4 and Table 2 present the results of the weight average molecular weight (M_w) and molecular weight distribution (MWD) of the bulk and the 3DOM PE samples with different pore sizes, respectively. It reveals that 3DOM PEs possess much higher M_w and broader MWD than the bulk one obtained under similar conditions. The high M_w of polymer achieved is possibly assigned to the effect of confined space, in which chain termination is hard to occur, thus the M_w of PE polymerized in inner space is higher than that in bulk space. The similar phenomena was also found in the literature [56], in which an ultrahigh molecular weight and a diameter of nanofibers PE were obtained by the polymerization of ethylene with a fibrous mesoporous silica supported titanocene catalyst in conjunction with MAO as a co-catalyst under high pressure (1 MPa). Compared with PE obtained from homogeneous catalyst in bulk polymerization, the broader MWD of 3DOM PE possibly arise from the heterogeneous characteristics of $Me_2Si[Ind]_2ZrCl_2/MAO$ catalysis system supported on the surface of silica template. Moreover, it can be found that the M_w of the 3DOM PE is increased with the size of silica microspheres reduced, which also confirms that confined space restricts the chain termination, and this restriction is more intense with the confined space reduced.

The DSC results for the 3DOM PE samples with different pore sizes and bulk PE are shown in Fig. 5 and Table 3. Both melting temperature (T_m) and the crystallinity of bulk PE are observed at 139.2 °C and 63.9%, respectively, higher than those of 3DOM PE samples. As for crystallization behavior, there are some differences with the literature [56], the growth of ethylene chains is severely confined in a direction due to the linear channels of mesoporous silica fibers, which induced the formed polyethylene fibers consisted predominantly of extended-chain crystals. On the contrary, we presume that the confined direction is multi-directions to the growth of ethylene chains in the interstitial voids of silica template, which possibly results in the lower crystallinity to the polyethylene fibers. Moreover, according to the previous reports [57–60], the strong polymer/inorganic interactions can restrict the mobility of the bound polymer chains and prevent the polymer from crystallizing. This may be responsible for the decrease of crystallinity and T_m of 3DOM PE compared with bulk PE. In addition, from Table 3, it can be found that the crystallinity and T_m of 3DOM PE-3 are obviously higher than those of the others, which should be attributed to the polymer/inorganic interactions weaker with confined space increased. The results further indicate that polymer/inorganic interactions effect on the crystallization of polymer.

Table 2
GPC results for bulk PE and the 3DOM PE samples with different pore sizes.

Sample	M_w ($\times 10^{-4}$)	MWD
bulk PE[a]	8.2	3.09
3DOM PE-1	47.2	9.5
3DOM PE-2	37.3	9.6
3DOM PE-3	29.1	7.4

[a] Experimental conditions: V (toluene) = 50 ml, $n(Al)/n(Zr) = 2000$, $n(Zr) = 2.0 \times 10^{-6}$ mol, $\theta = 30$ min, $T = 60$ °C, $P = 0.1$ MPa.

Table 3
DSC results for bulk PE and the 3DOM PE samples with different pore sizes.

Sample	T_m (°C)	Crystallinity (%)
bulk PE	139.2	63.9
3DOM PE-1	134.0	41.2
3DOM PE-2	135.3	43.4
3DOM PE-3	137.4	55.6

4. Conclusion

A convenient and friendly method was offered to fabricate 3DOM PE with pore size in the range of 135–410 nm *via* infiltration and then polymerization of gaseous ethylene. SEM micrographs show that the pores are uniform, flexible and arranged in a highly ordered fashion. Optical characterization also confirmed the uniform nature of the 3DOM PE. The properties of 3DOM PE with different pore sizes were characterized by GPC and DSC. GPC results show that the porous PE possesses higher M_w and broader MWD compared with bulk PE, and the M_w of the 3DOM PE is increased with the size of silica microspheres reduced, which also indicates that confined space restricts the chain termination, and this restriction becomes more intense as the confined space reduced. Moreover, DSC results reveal that 3DOM PE exhibits lower melting temperature and crystallinity than those of bulk PE due to the effect of polymer/inorganic interactions.

Acknowledgement

This work was supported by the National Natural Science Foundation of China (no. 50273009); the Natural Science Foundation of Hebei Province (no. E2007000052); Education Department Science Research Plan of Hebei Province (no. 2007307); and Doctor Open Foundation of Key Laboratory of Functional Polymer Material (Nankai University) of Education Ministry (no. 2006-007).

References

[1] Joannopoulos JD, Villeneuve PR, Fan S. Nature 1997;386:143.
[2] Jiang P, Hwang KS, Mittleman DM, Bertone JF, Colvin VL. J Am Chem Soc 1999;121:11630.
[3] Dong W, Bongard HJ, Marlow F. Chem Mater 2003;15:568.
[4] Saravanamuttu K, Blanford CF, Sharp DN, Dedman ER, Turberfield AJ, Denning RG. Chem Mater 2003;15:2301.
[5] Qian W, Gu ZZ, Fujishima A, Sato O. Langmuir 2002;18:4526.
[6] Lee YJ, Braun PV. Adv Mater 2003;15:563.
[7] Takeoka Y, Watanabe M. Langmuir 2002;18:5977.
[8] Scott RWJ, Yang SM, Chabanis G, Coombs N, Williams DE, Ozin GA. Adv Mater 2001;13:1468.
[9] Lewandowski K, Murer P, Svec F, Fréchet JMJ. Anal Chem 1998;70:1629.
[10] Akolekar DB, Hind AR, Bhargava SK. J Colloid Interface Sci 1998;199:92.
[11] Tanev PT, Chibwe M, Pinnavaia TJ. Nature 1994;368:321.
[12] Deleuze H, Schultze X, Sherrington DC. Polymer 1998;39:6109.
[13] Wang H, Li XD, Hong LY, Kim DP. J Porous Mater 2006;13:115.
[14] Wu QZ, Yin Q, Liao JF, Deng JH, Li YG. Chin J Chem 2005;23:689.
[15] Tennikov MB, Gazdina NV, Tennikova TB, Svec F. J Chromatogr A 1998;798:55.
[16] Palm A, Novotny MV. Anal Chem 1997;69:4499.
[17] Xie S, Svec F, Fréchet JMJ. J Chromatogr A 1997;775:65.
[18] Wijnhoven JEGJ, Zevenhuizen SJM, Hendriks MA, Vanmaekelbergh D, Kelly JJ, Vos WL. Adv Mater 2000;12:888.
[19] Kulinowski KM, Jiang P, Vaswani H, Colvin VL. Adv Mater 2000;12:833.
[20] Chi EO, Kim YN, Kim JC, Hur NH. Chem Mater 2003;15:1929.
[21] Bartlett PN, Dunford T, Ghanem MA. J Mater Chem 2002;12:3130.
[22] Yang L, Cao W. Chem Mater 2006;18:297.
[23] Norris DJ, Vlasov YA. Adv Mater 2001;13:371.
[24] Luo Q, Liu Z, Li L, Xie S, Kong J, Zhao D. Adv Mater 2001;13:286.
[25] Davis ME. Nature 2002;417:813.
[26] Park SH, Xia Y. Chem Mater 1998;10:1745.
[27] Gates B, Yin Y, Xia Y. Chem Mater 1999;11:2827.
[28] Bartlett PN, Birkin PR, Ghanem MA, Toh CS. J Mater Chem 2001;11:849.
[29] Park SH, Xia Y. Adv Mater 1998;10:1045.
[30] Cassagneau T, Caruso F. Adv Mater 2002;14:34.
[31] Mclachlan MA, Johnson NP, De La Rue RM, Mccomb DW. J Mater Chem 2004; 14:144.
[32] Bu HT, Rong JH, Yang ZZ. Macromol Rapid Commun 2002;23:460.
[33] Xia Y, Gates B, Yin YD, Lu Y. Adv Mater 2002;12:693.
[34] Yan WD, Li HQ, Shen X. Macromol Rapid Commun 2005;26:564.
[35] Zhang X, Yan WD, Li HQ. Polymer 2005;46:11958.
[36] Yan WD, Li HQ, Shen X. Eur Polym J 2005;41:992.
[37] Velev OD, Jede TA, Lobo RF, Lenhoff AM. Nature 1997;389:447.
[38] Imhof A, Pine DJ. Nature 1997;389:948.
[39] Holland BT, Blanford CF, Stein A. Science 1998;281:538.
[40] Wijnhoven JEGJ, Vos WL. Science 1998;281:802.
[41] Zakhidov AA, Baughman RH, Iqbal Z, Cui C, Khayrullin I, Dantas SO, et al. Science 1998;282:897.
[42] Míguez H, Blanco A, Meseguer F, López C, Yates HM, Pemble ME, et al. Phys Rev B 1999;59:1563.
[43] Blanco A, Chomski E, Grabtchak S, Ibisate M, John S, Leonard SW, et al. Nature 2000;405:437.
[44] Sötber W, Fink A. J Colloid Interface Sci 1968;26:62.
[45] Chien JCW, He D. J Polym Sci A Polym Chem 1991;29:1603.
[46] Soga K, Kaminaka M. Makromol Chem 1993;194:1745.
[47] Soga K, Shiono T, Kim HJ. Makromol Chem 1993;194:3499.
[48] Soga K, Kaminaka M. Makromol Chem Rapid Commun 1992;13:221.
[49] Kaminaka M, Soga K. Makromol Chem Rapid Commun 1991;12:367.
[50] Kaminaka M, Soga K. Polymer 1992;33:1105.
[51] Kaminsky W, Rener F. Makromol Chem Rapid Commun 1993;14:239.
[52] Collins S, Kelly WM, Holden DA. Macromolecules 1992;25:1780.
[53] Chen YX, Rausch MD, Chien JCW. J Polym Sci A Polym Chem 1995;33:2093.
[54] Rong JH, Yang ZZ. Macromol Mater Eng 2002;287:11.
[55] Russell TP. Science 2001;293:446.
[56] Kageyama K, Tamazawa J, Aida T. Science 1999;285:2113.
[57] Nakajima H, Yamada K, Iseki Y, Hosoda S, Hanai A, Oumi Y, et al. J Polym Sci B Polym Phys 2003;41:3324.
[58] Tsagaropoulos G, Eisenberg A. Macromolecules 1995;28:6067.
[59] Vaia A, Sauer RBB, Tse OK, Giannelis EP. J Polym Sci B Polym Phys 1997; 35:59.
[60] Maiti P, Nam PH, Okamoto M, Hasegawa H, Usuki A. Macromolecules 2002; 35:2042.